The application of Helmholtz resonance to determination of the volume of solids, liquids and particulate matter

A thesis presented in partial fulfilment of the requirements for the degree of
Doctor of Philosophy
in
Instrumentation and Process Engineering

At Massey University, Palmerston North
New Zealand

Emile Stefan Webster

November
2010

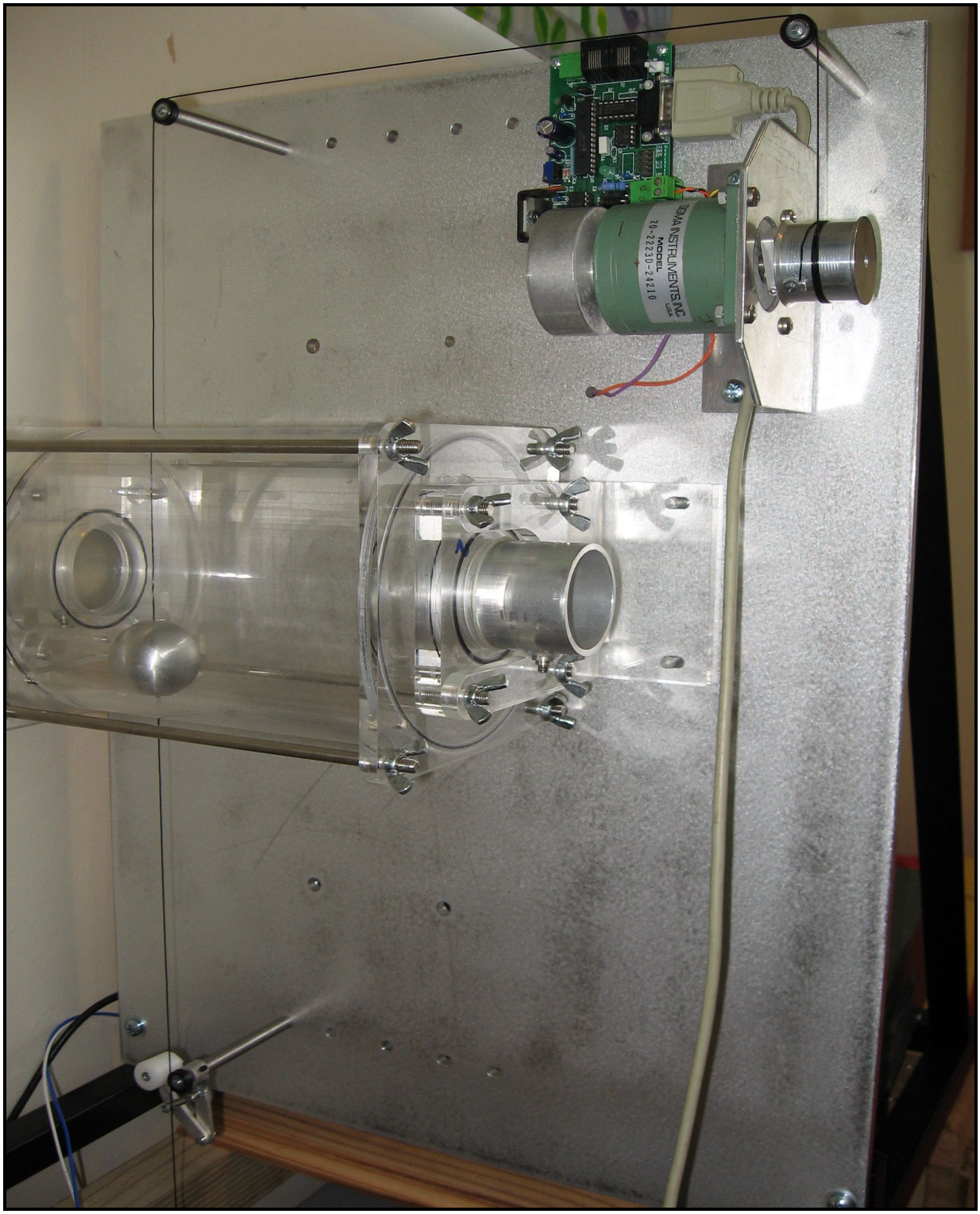

Pulley apparatus set up for mapping the resonant frequency versus sample location in the horizontal configuration

Abstract

The aim of this investigation was the creation of a high precision volume measurement device using the Helmholtz resonator principle, the purpose of which was to measure, without interference, liquids, solids and particulate samples. A previous study by Nishizu *et al.* (2001) suggested they achieved an accuracy of about ±1% of full scale, where full scale is 100% fill of the resonator chamber. Theory suggested that with careful design and measurement accuracy of approximately ±0.1% should be achievable.

A high precision resonator was designed using acoustic theory and drawn using SolidWorks™ computer aided design software. This was then built using a computerised numerical controlled milling machine. The resulting resonator was coupled to a 16-bit high-speed data acquisition system driven by purpose-made LabVIEW™ software. Using a resonant hunting method, repeatability was within ±1mL for a 3L chamber and the accuracy was better than ±3mL, which is ±0.1% of full scale for liquid and solid samples.

Testing of particulate material gave results indicating complex behaviour occurring within the resonator. Accuracy of sub-millimetre granular samples was restricted to approximately ±1%, and fill factors to about 50%. This reduction in accuracy was caused by a combination of energy absorption and resonant peak broadening. Medium sized particles, between 1mm and 15mm allowed measurement accuracies of approximately ±0.5%. Larger samples, greater than 15mm in diameter, gave results with comparable accuracy to water and solids tested.

It was found that most materials required a post measurement curve fit to align predictive volume calculations. All samples were observed to have a predictive deviation curve with coefficients dependent on the material or general shape. This curve appeared to be a function of sample regularity and/or whether the sample has interstitial spaces. To achieve high measurement accuracy temperature compensation was required to negate drifts in sample measurement.

Chamber mapping was conducted using a spherical solid moved to precise locations, then making a three-dimensional frequency map of the inside of a dual port resonator. This showed the length extension term for the moving mass of air in the port penetrates roughly three times further than theory suggests. However, the influence of this extra ‘tail’ was found to be negligible when calculating sample volumes.

A new method of measuring volume was developed using Q profile shifting and ambient temperature information. Accuracies for this method were comparable to those found using the resonant hunting method. A significant advantage of the new method is a 2-3 second measurement time compared to approximately 40 seconds for the resonant hunting method. The Q profile shifting method allowed volume measurements on samples moving through a dual port resonator at speeds of up to 100mm/s.

Free fall measurements proved unsuccessful using existing methods, but variations in signal data for different sample sizes suggest the need for future investigation.

Follow-up studies may provide new interpretation models and methods for high-speed acquisition and analysis required to solve freefall measurements.

Precise temperature (speed of sound) and flange factor (responsible for port length extension) relationships were evaluated. The correction factor for the speed of sound with temperature was found to be marginally different to established theory using the Helmholtz equation due to temperature secondary effects in the port length extension factor. The flange factor, which determines port length extension, for the configurations used in this investigation was experimentally found to be approximately 5% less than theoretical values.

It was established that the sample to be measured must be within a certain region of the chamber for accurate volume measurements to be made. If the sample were larger than the bounded region the resonant frequency would no longer obey the Helmholtz relationship. This would thereby reduce the accuracy of the measurement. All samples irrespective of cross sectional area were found to alter the resonant frequency when they were over 85% of the chamber height.

An equalisation method termed environmental normalisation curve was developed to prevent environmental and loudspeaker deficiencies from colouring Q profiles used in Q profile shifting procedures. This was undertaken as Q profile shifting relies on consistency in the Q profile. The environmental normalisation curve was able to equalise external factors to within $\pm$0.4dB. The environmental normalisation method could be used to post-process data or applied in real time to frequency generation.

The controlled decent Q profile shifting technique was refined further to be used in continuous measurements in a single port resonator. Samples could theoretically be measured up to 15% of full-scale fill before resonant peak predictability would compromise accuracy. Measurement times were from one to three seconds, depending on environmental temperature stability.

An alternative Helmholtz resonator was developed and investigated using an inverted port. This variant has potential applications for a seal-less chamber and port with rapid non-interference chamber access. Q factors for the inverted port resonator were found to be significantly less than tradition Helmholtz resonators. It is believed this is due to a larger boundary layer acoustic resistance occurring in the inverted port.

A variable chamber resonator was designed and built as a further development of the Helmholtz resonator volume measurement system, as the uncertainty of measurement is a function of resonant chamber size. Therefore, using the variable chamber resonator the chamber size could be customised to the sample size. In this way the uncertainty of measurement could be minimised. The variable chamber resonator was used with both the resonant hunting method and the Q profile shifting method.

Volume measurements on produce and minerals using the variable chamber resonator yielded results of similar accuracy to measurements on calibration samples. Each sample type displayed characteristics that would make specific calibration necessary. Both techniques were able to detect hidden void spaces, larger than 2% of the sample volume, and in punctured samples. Therefore, both methods may be viable for rapid sorting of produce and minerals.

Acknowledgements

I would like to thank my supervisor, Professor Clive Davies, for his continued encouragement throughout my course of study, providing opportunities for personal development and assistance in attaining scholarships and funding for this investigation.

I would like to thank my wife, Nadia, for her support in allowing me the time to conduct this thesis and her tireless efforts in proof reading and editing early drafts.

Thanks also to Steve Tallon (PhD), co-supervisor, for his help in reading and critiquing later drafts. Thanks also for help in gaining access to Industrial Research LTD (IRL) anechoic facilities and instruments used for calibration purposes.

Lastly I would like to thank the workshop services at the Massey University Wellington campus, especially Mike Turner for his excellent work in fabricating the various resonator components, pulley apparatus and variable chamber resonator.

Table of contents

Figures and Tables

Nomenclature

a	Primary radius , polynomial coefficient (with subscript)	(m)
BL	Boundary layer	(m)
c	Speed of sound	(m/s)
c_p	Specific heat, constant pressure	(J/kg.K)
c_v	Specific heat, constant volume	(J/kg.K)
c_0	Speed of sound (STP)	(m/s)
d	Diameter	(m)
D	Energy density	(W.s/m^3)
f	Force	(N)
$freq$	Frequency	(Hz)
i	Complex notation	-
I	Intensity	(W/m^2)
k	Wave number	($k = \omega/c$)
L	Length	(m)
l_p	Port length	(m)
l_p'	Total port length	(m)
L_{mfp}	Mean free path length	(m)
Δl	Port length extension	(m)
m	Mass	(kg)
M	Mean molecular weight	(kg)
M_{mol}	Molar mass	(kg)
n	Number of moles	-
N	Number of molecules	-
p	Particular pressure	(Pa)
p_0	Pressure at STP	(Pa)
P_0	Primary pressure	(Pa)
δp	Excess pressure	(Pa)
P_r	Prandtl number	-
Q	Quality factor	-
Q_s	Strength of source	-
r	Primary distance from source	(m)
R	Secondary distance from source, Reflection ()	(m)
R_a	Acoustic resistance	(N.m/s^5)
R_m	Mechanical resistance	(N.m/s)
R_r	Radiation resistance	(N.m/s)
R_{eflect}	Reflective coefficient	-
R_c	Gas constant	(8.31 J/mol.K)
R_N	Reynolds number	-
S	Surface	(m^2)
s	Cross sectional area	(m^2)
ST	Sweep time	(s)
t	Time	(s)
T	Wave period	(s)
T_{emp}	Temperature	(K)
$T_{ransmit}$	Transmission coefficient	
U_0	Primary velocity	(m/s)
U_s	Specific velocity	(m/s)
U_v	Volume velocity	(m^3/s)

V	Volume	(m^3)
w	Sample volume	(m^3)
X_a	Acoustic reactance	($N.m/s^5$)
X_m	Mechanical reactance	(N.m/s)
X_r	Radiation reactance	(N.m/s)
Y	Thermal conductivity	(W/m.K)
Z	Characteristic impedance	($N.m/s^3$)
Z_a	Acoustic impedance	($N.m/s^5$)
Z_m	Mechanical impedance	(N.m/s)
Z_r	Radiation impedance	(N.m/s)
Z_s	Specific impedance	($N.m/s^3$)

Greek symbols

α	Helmholtz equation constant	(Hz/K)
β	Temperature gradient compensation	-
δ	Length extension factor	(m)
γ	Adiabatic gas ratio	(c_p/c_v)
θ	Primary angle	(radians)
λ	Wavelength	(m)
μ	Viscosity	($N.s/m^2$)
ρ	Particular air density	(kg/m^3)
ρ_0	Density at STP	(kg/m^3)
$\delta\rho$	Excess density	(kg/m^3)
ς	Power reflective coefficient	-
σ	Secondary radius	(m)
τ	Power transmission coefficient	-
ν	Kinematic viscosity	(m^2/s)
v_{rms}	Root mean squared velocity	(m/s)
φ	Secondary Angle	(radians)
ψ	Tertiary angle	(radians)
ω	Angular frequency	(radians/s)
Ω	Approximation function	-

Subscripts

+	Incident	-	Reflected
0	Initial value	*1,2*	Later values, coefficient number
c	Chamber	*e*	Extension
H	High	*i*	inner
n	Value in	*inst*	Instantaneous
L	Low	*max*	Maximum
min	Minimum	*o*	outer
Out	Value out	*p*	Port
t	Transmitted	*T*	Temperature
Therm	Thermal	*Visc*	Viscous

Vector quantities are represented by either a cap or in **bold**.

Basic equations

Particular pressure: $p = \rho_0 c U_0$ (1)

Volume velocity: $U_v = S U_s$ (2)

Acoustic impedance: $Z_a = p / U_v = Z_s / s_p$ (3)

Specific impedance: $Z_s = p / U_s$ (4)

Mechanical impedance: $Z_m = f / U_s$ (5)

Radiation impedance: $Z_r = Z_a s_p{}^2 = Z_s s_p$ (6)

Characteristic impedance: $Z = \rho_0 c$ (7)

Acoustic intensity for a sphere: $I = p^2 / 2\rho_0 c$ (8)

Acoustic power for a sphere: $W = 4\pi a^2 I$ (9)

Sound energy density: $D = p^2 / \rho_0 c^2 = p^2 / \gamma p_0$ (10)

Acoustic intensity level (dB): $Intensity = 10\log_{10}\left(\frac{I_{out}}{I_{in}}\right)$ (11)

Acoustic power level (dB): $power = 10\log_{10}\left(\frac{W_{out}{}^2}{\rho_0 c}\frac{\rho_0 c}{W_{in}{}^2}\right)$ (12)

Specific resistance derivation: $power = 10\log_{10}\left(\frac{W_{out}{}^2}{R_s{}^{out}}\frac{R_s{}^{in}}{W_{in}{}^2}\right)$ (12a)

$$power = 20\log_{10}\left(\frac{W_{out}}{W_{in}}\right) + 10\log_{10}\left(\frac{R_s{}^{in}}{R_s{}^{out}}\right)$$

Sound pressure level (dB): $power = 20\log_{10}\left(\frac{p}{p_{ref}}\right)$ (13[1])

Excess pressure: $\delta p = p - p_0$ (14)

[1] P_{ref} is a predefined reference pressure of $2x10^{-5}$Pa for hearing and liquids or 0.1Pa for transducer calibration.

Excess density: $\delta\rho = \rho - \rho_0$ (15)

The specific velocity: $U_s = U_0 e^{i\omega t}$ (16)

The specific pressure: $p = P_0 e^{i\omega t}$ (17)

Strength of spherical Source: $Q_s = 4\pi a^2 U_0$ (18)

Forward travelling wave: $p = ZU_s$ (19)

Backward travelling wave: $p = -ZU_s$ (20)

Standard Helmholtz equation

$$\omega_{res} = 2\pi freq = c\sqrt{\frac{s_p}{(V-w)(l_p + \Delta l)}} \quad (21)$$

Sample volume Helmholtz equation

$$w = V - \frac{s_p}{(l_p + \Delta l)\left(\frac{2\pi freq}{\beta c}\right)^2} \quad (22)$$

Temperature correction for speed of sound

$$c_0 = \sqrt{\gamma \frac{p_0}{\rho_0}} = \sqrt{\frac{\gamma R_c T_{emp}}{M}} \quad (23)$$

Measured Q factor equation $Q = \frac{\omega}{(\omega_H - \omega_L)}$ (24)

Theoretical Q factor for a Helmholtz resonator

$$Q = \frac{\omega m}{R_m} = 2\pi\sqrt{\frac{{l_p}^3 V}{{s_p}^3}} \quad (25)$$

Glossary

Attenuation	Difference in sound pressure level between two points
BL	Boundary Layer
BEM	Boundary Element Model
Chamber	Main body of resonator in which sample volume is measured
Characteristic impedance	Measure of acoustic resistance in the far field
Chirp	A narrow frequency sweep
CSA	Cross Sectional Area
dB	Decibels, measure of relative sound level
ENC	Environmental Normalisation Curve
Excess pressure	Differential pressure to the density at STP
Excess density	Differential density to the density at STP
Far field	Distance at which sound level is uniform
Flange factor	Multiplying factor for determining port length extension
FFT	Fast Fourier Transform
FEM	Finite Element Model
Helmholtz resonator	Resonator consisting of chamber and port
Interstitial space	Space between adjacent particles in a granular bed
IIR	Infinite Impulse Response (Digital filter)
Length extension	Extra distance the air in port moves beyond physical port length
Mechanical impedance	Combined mechanical resistance and reactance
Mechanical resistance	Sum of all real resistive components in the resonant system
Mechanical reactance	Sum of all imaginary force components in the resonant system
Near field	Distance where localised effects make sound levels non-uniform
Neck	Alternative name for port
Particular pressure	The instantaneous pressure of an oscillatory pressure wave
Pink noise	Random frequencies having equal power
Port	Tube of smaller *CSA* than chamber connecting chamber to a secondary impedance region (usually an open environment)
Primary pressure	The maximum pressure in an oscillatory pressure wave
Primary velocity	The maximum velocity in an oscillatory wave
Q factor	Quality factor, quality of resonance
QPS	Q Profile Shifting
Radiation impedance	Combined radiation resistance and reactance
Radiation resistance	Measure of the real resistive losses from the port
Radiation reactance	Measure of the imaginary forces in the port
Reflective coefficient	Reflected component based on the ratio change of two impedance mediums
RMS	Root Mean Squared (geometric average)
RTD	Resistive Temperature Device
Specific velocity	The instantaneous velocity of an oscillatory wave

SPL	Sound Pressure Level (dB)
STP	Standard Temperature and Pressure ($15^{o}C$, $1.01x10^{5}Pa$)
SWR	Standing Wave Ratio (maximum over minimum pressure)
Transmission coefficient	Transmitted component based on the ratio change of two impedance mediums
VCR	Variable Chamber Resonator
White noise	Random frequencies having random power